Nonlinear edge modes from topological one-dimensional lattices

Lucien Jezequel and Pierre Delplace
Univ Lyon, ENS de Lyon, CNRS, Laboratoire de Physique, F-69342 Lyon, France

(Received 21 July 2021; accepted 14 December 2021; published 11 January 2022)

We propose a method to address the existence of topological edge modes in one-dimensional (1D) nonlinear lattices, by deforming the edge modes of linearized models into solutions of the fully nonlinear system. For sufficiently large nonlinearites, the energy of the modified edge modes may eventually shift out of the gap, leading to their disappearance. We identify a class of nonlinearities satisfying a generalized chiral symmetry where this mechanism is forbidden, and the nonlinear edge states are protected by a topological order parameter. Different behaviors of the edge modes are then found and explained by the interplay between the nature of the nonlinearities and the topology of the linearized models.

DOI: 10.1103/PhysRevB.105.035410

Since the discovery of the quantum Hall effect [1], the number of physical systems exhibiting topological boundary modes has been constantly increasing. Originally found in condensed matter, robust edge states are now found in virtually all wave systems [2–4] showing the ubiquity of topological edge modes independently of their physical implementation. The robustness of the edge modes is understood through the celebrated bulk-boundary correspondence that relates the number of edge modes to a topological invariant of the bulk bands as long as the spectrum is gapped [5–8].

From the beginning, the theory of topological edge modes has been tied to linear systems concepts such as eigenmodes and energy spectra. Actually, many platforms used to implement those topological properties, such as polaritons, photonic lattices, fluids, and networks of springs and electric circuits, also naturally exhibit nonlinear behaviors. This recently stimulated a growing interest in the interplay of topology with nonlinearities [9–11], with applications to topological lasing [12,13] and topological synchronization [14]. Regarding the edge states in nonlinear systems, investigations in specific cases showed the existence of nonlinear bulk and edge solitons with some similarities with the linear case [15–21]. In some examples in one dimension (1D), the energy of the edge modes was found to depend on the amplitude [16,19,22–24], while in others, the energy was found to be fixed [17,18,25]. These results suggest that the concept of stationary topological edge mode seems generalizable to the nonlinear realm, with, however, a lack of a systematic theoretical understanding that goes beyond the scope of sporadic examples.

In this work, we provide criteria for the existence of nonlinear topological edge states. We focus on nonlinear Schrödinger equations on 1D lattices, whose nonlinear Hamiltonian H_ψ splits into a linear topological part H_{topo} and a nonlinear one $H_{\psi,\text{NL}}$ as

$$i\partial_t |\psi\rangle = H_\psi |\psi\rangle = (H_{\text{topo}} + H_{\psi,\text{NL}}) |\psi\rangle . \tag{1}$$

The burning question to ask is then the following: What are the conditions for the edge states of the linear topological model H_{topo} to survive the presence of nonlinearities $H_{\psi,\text{NL}}$? To answer this question, we propose a method based on exact perturbation theory that generates the edge modes and their energy of nonlinear systems of the form (1). The idea is to start with the edge mode of the linearised system at small amplitude and then increase smoothly the amplitude of the mode. As the relative strength of the nonlinearities increases, we are then able to deform the initial linear edge mode in a way that it remains a stationary edge solution of the nonlinear dynamics. The method can eventually reach nonlinear edge modes with a high amplitude as long as their energy remains in the spectral gap of the linearized dynamics. If this condition stops being fulfilled, the nonlinear edge state is then quickly delocalized into the bulk [19] and becomes unstable [26]. Then, we extend the notion of chiral symmetry to nonlinear systems and show that chiral symmetric nonlinearities prevent such a delocalization, thus protecting the nonlinear edge state. We then characterize those robust nonlinear edge modes with a local topological index. Our theory is illustrated with two nonlinear generalizations of the Su-Schrieffer-Heeger (SSH) model—one being chiral and one which is not—and confirmed numerically.

A concrete situation where the nonlinear Schrödinger equation modifies a 1D topological lattice model is that of an SSH chain with couplings t_1 and t_2 between nearest neighbors and an on-site Kerr-like nonlinearity [11,16] similar to those appearing in the Gross-Pitaevskii equation for Bose-Einstein condensates [27]:

$$\begin{cases} i\partial_t a_j = t_1 b_j + t_2 b_{j-1} + |a_j|^2 a_j \\ i\partial_t b_j = t_1 a_j + t_2 a_{j+1} + |b_j|^2 b_j . \end{cases} \tag{2}$$

A state $|\psi\rangle$ of the system can be decomposed in the basis of the two sublattices as

$$|\psi\rangle = \begin{pmatrix} |\psi_A\rangle \\ |\psi_B\rangle \end{pmatrix} = \begin{pmatrix} \sum_j a_j |j,A\rangle \\ \sum_j b_j |j,B\rangle \end{pmatrix}, \tag{3}$$

where j labels the unit cell. The application of H_ψ to such a state then gives the vector $H_\psi\,|\psi\rangle$ which expands as

$$H_\psi\,|\psi\rangle = \begin{pmatrix} \sum_j (t_1 b_j + t_2 b_{j-1} + |a_j|^2 a_j)\,|j,A\rangle \\ \sum_j (t_1 a_j + t_2 a_{j+1} + |b_j|^2 b_j)\,|j,B\rangle \end{pmatrix} \tag{4}$$

for the model (2). The linear SSH model is recovered when $|\psi\rangle$ is small in amplitude. In that case, this model is known to have a gap in energy around $E = 0$ when $|t_1| < |t_2|$, except for stationary topological edge modes which are localized at each end of the chain [28,29]. We then would like to know how these edge modes survive the introduction of the nonlinearities, such as in (4). We show below that edge states exist in nonlinear Schrödinger models when three conditions are met:

(i) The linearized model has an edge state which is in the gap of the bulk bands.

(ii) The differential of H_ψ around any state $|\psi\rangle$ is Hermitian, i.e., $dH_\psi^\dagger = dH_\psi$.

(iii) The nonlinear Hamiltonian H_ψ verifies the $U(1)$-symmetry $H_{e^{i\phi}\psi}(e^{i\phi}\,|\psi\rangle) = e^{i\phi} H_\psi\,|\psi\rangle$ for all $|\psi\rangle$.

Assumption (i) is quite natural, as we search nonlinear edge states as resulting from the deformation of linear ones. Assumption (ii) is made to guarantee that the energy E of the state remains real, and assumption (iii) is needed to ensure that finding nonlinear states of real energy $E\,|\psi\rangle = H_\psi\,|\psi\rangle$ also generates solutions of (1) of the form $|\psi(t)\rangle = |\psi\rangle\, e^{-iEt}$. Note that our model (2) satisfies these three conditions. Note that those general hypothesis do not depend on the order of the nonlinear terms. Our method is thus not specific to Kerr-like terms and applies to arbitrary nonlinearities as long as the three hypotheses above are satisfied.

We now provide an explicit method to construct the nonlinear edge modes assuming that the three conditions above are met. For that, let us study the space of edge states $|\psi\rangle$ of energy E of H_ψ that we define as being spanned by the doublet $(E, |\psi\rangle)$. The key idea to explore this space is to parametrize it with a continuous parameter s and to derive the evolution equation for the states close in s. If $(E_s, |\psi_s\rangle)$ is a doublet such that for all s, $|\psi_s\rangle$ is a solution of

$$E_s\,|\psi_s\rangle = H_\psi\,|\psi_s\rangle \tag{5}$$

and then, by differentiating this equation along s, one finds that the condition for this path to exist is to satisfy the following evolution equation:

$$(dH_{\psi_s} - E_s)\,|\partial_s\psi_s\rangle = (\partial_s E_s)\,|\psi_s\rangle\,, \tag{6}$$

where the differential dH_ψ is a linear operator that describes the variation of H_ψ for a small perturbation $|\partial_s\psi\rangle$ around $|\psi\rangle$. One can thus interpret it as an effective Hamiltonian $H_{\text{eff},s} \equiv dH_{\psi_s}$ when linearizing around $|\psi_s\rangle$.

The free variables of (6) are $|\partial_s\psi_s\rangle$ and $\partial_s E_s$. It follows that for a lattice with n sites, (6) is a system of n differential equations with $n+1$ variables. Thus, at fixed s, the space of solutions $(\partial_s E_s, |\partial_s\psi_s\rangle)$ of (6) is a vector space of dimension at least one. Therefore, there exists (at least) a solution to our evolution equation. Moreover, hypothesis (ii) implies that there is solution with $\partial_s E_s$ real. One can therefore reconstruct from (6) the continuous family of stationary solutions $(E_s, |\psi_s\rangle)$ of (5) along this path, given an initial condition at $s = 0$, that we choose to be $(E_{s=0}, |\psi_{s=0}\rangle) = (0, 0)$.

For an infinitesimal deviation away from this initial condition, H_ψ can be linearized as $H_{\text{eff},0} = dH_0$. If this linear model hosts at least one edge mode of zero-energy $|\psi\rangle$, like in the SSH model, then $((\partial_s E_s)_{s=0} = 0, |\partial_s\psi_s\rangle_{s=0} = |\psi\rangle)$ is a valid solution of (6) for $s = 0$. Solving this differential system, one can therefore generate nonlinear edge states $|\psi_s\rangle$ with a growing amplitude as s increases. If the linear model hosts multiple zero-energy edge modes as the SSH model (one on each edge), all of them could be used for the dynamic, leading to different nonlinear edge modes.

So far, we have obtained the existence of solutions $(\partial_s E_s, |\partial_s\psi_s\rangle)$ for (5) but we have not shown yet that they remain localized near the edge. The question is the following: If the linear model at $s = 0$ has an edge mode, is $|\psi_s\rangle$ also localized near the edge for $s > 0$? In systems where coupling constants between sites decay quickly with their distance as in our illustrative nonlinear SSH model (2), the answer is given by the Combes-Thomas theorem [30,31]. This theorem states that solutions $|\partial_s\psi_s\rangle$ of (6) are localized around $|\psi_s\rangle$ as long as E_s lies in the bulk gap of $H_{\text{eff},s}$. If this condition stops being satisfied, $|\psi_s\rangle$ can quickly be delocalized as $|\partial_s\psi_s\rangle$ starts to strongly resonate with the nearby bulk modes.

In most cases, the system (6) must be solved numerically, using standard algorithmic methods [32]. In particular, we can solve this system for the Kerr-like nonlinear SSH model (2) as an illustration. As this is a model which verifies the general hypotheses (i)–(iii), we can therefore generate left edge states with a growing amplitude as s increases (see Fig. 1). For small amplitude, their shape remains close to the exponential shape of the edge states of the linearized model. But as the relative strength of the nonlinearities increase, the nonlinear edge states become more deformed. In particular, we observe that the nonlinear edge states become less localized as their energy E_s approaches the bulk bands of $H_{\text{eff},s}$. Around $s \approx 1.5$ the energy touches those bands and the edge state becomes strongly delocalized. Therefore, the edge state is not topologically protected in the strong amplitude regime. Moreover, since the system is nonlinear, one can ask about the stability of such stationary solutions under small perturbations [19,26,33]. In order to do so, we add a random perturbation $|\delta\psi\rangle$ to a stationary solution $|\psi_s\rangle$. Then, for the initial condition $|\psi(t=0)\rangle = |\psi_s\rangle + |\delta\psi\rangle$, we evaluate how far the solution $|\psi(t)\rangle$ of (1) deviates from the original stationary solution $|\psi_s\rangle$ by measuring the time evolution of their distance $\| \,|\psi(t)\rangle - |\psi_s\rangle\, \| = \sum_j |\psi_j(t) - \psi_{s,j}|$, where ψ_i denotes the i-site amplitude. If the deviation grows exponentially with time, the state is unstable. We find (see Fig. 1) that the edge state is stable as long as the energy E_s does not enter the bulk bands, which occurs at about $s \approx 1.2$–1.5. Beyond this threshold, the states $|\psi_s\rangle$ become strongly unstable, highlighting again the criticality of this regime.

In practical situations, one would like to prevent this band touching to occur by constraining the energy at zero, in the middle of the gap of $H_{\text{eff},s}$. In 1D insulators, this protection role is made by the presence of a chiral symmetry. To follow that spirit, we introduce a generalization of the chiral symmetry to nonlinear systems. This allows us to identify nonlinearities that forbid the energy shift and therefore host

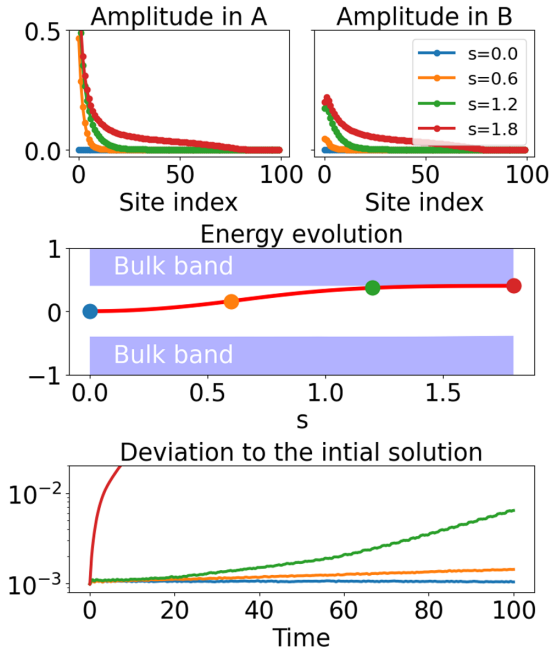

FIG. 1. Numerical resolution of (6) for the left edge modes of model (2). We work with 100 pairs of sites and the constants $t_1 = 0.6$ and $t_2 = 1$. The amplitude of ψ_s is given on the sites of type A (upper left) and B (upper right) for different s. (Center) The evolution of the energy E_s of ψ_s is drawn in red and the bulk bands of $H_{\text{eff},s}$ in light blue. (Bottom) Deviation $\| |\psi(t)\rangle - |\psi_s\rangle \|$ between the stationary solution $|\psi_s\rangle$ and an initially perturbed one by a random vector of norm 10^{-3}, for different values of s.

edge states that are robust and topologically protected. Besides, unlike the general case discussed so far, the result does not require H_ψ to satisfy a $U(1)$ symmetry, nor dH_ψ to be Hermitian.

We say that a nonlinear operator H_ψ satisfies a chiral symmetry if there is a bipartition A and B of the degrees of freedom—e.g., two sublattices—such that the state $H_\psi |\psi\rangle$ decomposes onto a single sublattice (say B) *if* $|\psi\rangle$ decomposes onto the other sublattice (say A). Put formally, one wants

$$|\psi\rangle_B = 0 \Rightarrow (H_\psi |\psi\rangle)_A = 0 \qquad \text{(same for } A \leftrightarrow B\text{)}. \tag{7}$$

In the linear case, (7) imposes H to be off-diagonal when written in the A and B basis. Our definition thus generalizes the chiral symmetry.

For the sake of concreteness, let us illustrate whether this symmetry is satisfied for a few different nonlinear terms. For the Kerr nonlinearity of the model (2), we have $H_{\text{Kerr},\psi} |\psi\rangle = \sum_j a_j^3 |j,A\rangle + b_j^3 |j,B\rangle$, so $(H_{\text{Kerr},\psi} |\psi\rangle)_A = \sum_j a_j^3 |j,A\rangle \neq 0$ even when $b_j = 0$. So the Kerr nonlinearity is not chiral symmetric. Instead, we can introduce the Kerr *intersite* nonlinearity, of the form $H_{\text{inter-Kerr},\psi} |\psi\rangle = \sum_j b_j^3 |j,A\rangle + a_j^3 |j,B\rangle$ that verifies $(H_{\text{inter-Kerr},\psi} |\psi\rangle)_A = \sum_j b_j^3 |j,A\rangle = 0$ when $|\psi\rangle_B = 0$ (meaning $b_j = 0\,\forall j$), and same for $A \leftrightarrow B$. This nonlinearity is thus chiral symmetric. As additional examples, we give below a list of nonlinear terms with general exponents α or β and classify them according to the chirality condition. It should be noted that this list stays valid if one does the exchange $A \leftrightarrow B$ everywhere.

$H_\psi \|\psi\rangle$	$a_j^\alpha \|j,A\rangle$	$b_j^\alpha \|j,A\rangle$	$a_{j+1}^\alpha b_j^\beta \|j,A\rangle$	$b_{j-1}^\alpha b_{j+1}^\beta \|j,A\rangle$
Chiral	No	Yes	Yes	Yes

Importantly, when H_ψ is chiral symmetric, an initial linear edge state $|\psi_{s=0}\rangle$ living on a given sublattice can evolve through (6) as a stationary solution $|\psi_{s>0}\rangle$ that remains on the same sublattice. Indeed, if $|\psi_s\rangle$ is a solution of (6) satisfying $|\psi_0\rangle = 0$ and $|\psi_s\rangle_B = 0$, $\forall s$, then by writing (6) by blocks while assuming $E_s = 0$, one obtains

$$\begin{pmatrix} H_{\text{eff,s}}^{AA} & H_{\text{eff,s}}^{AB} \\ H_{\text{eff,s}}^{BA} & H_{\text{eff,s}}^{BB} \end{pmatrix} \begin{pmatrix} |\partial_s \psi_s\rangle_A \\ 0 \end{pmatrix} = 0, \tag{8}$$

$$|\psi\rangle = \begin{pmatrix} |\psi_A\rangle \\ 0 \end{pmatrix}. \tag{9}$$

Differentiating the condition (7) along the variable $|\psi\rangle_A$ yields $H_{\text{eff},s}^{AA} = 0$, so (8) reduces to

$$H_{\text{eff,s}}^{BA} |\partial_s \psi_s\rangle_A = 0. \tag{10}$$

In order to know whether $H_{\text{eff,s}}^{BA}$ has localised zero modes for each s, we use the theory of topological indices. For that purpose, we define the following operators in the spirit of super-symmetric approaches [34–36]

$$H'_{\text{eff,s}} = \begin{pmatrix} 0 & H_{\text{eff,s}}^{BA} \\ H_{\text{eff,s}}^{BA\,\dagger} & 0 \end{pmatrix}, \qquad C = \begin{pmatrix} \mathbb{1}_A & 0 \\ 0 & -\mathbb{1}_B \end{pmatrix}, \tag{11}$$

$$C = \begin{pmatrix} \mathbb{1}_A & 0 \\ 0 & -\mathbb{1}_B \end{pmatrix}, \qquad H = \begin{pmatrix} 0 & H^{BA} \\ H^{BA\dagger} & 0 \end{pmatrix}, \tag{12}$$

so that $\{H'_{\text{eff,s}}, C\} = 0$, implying that $H'_{\text{eff,s}}$ is a chiral Hermitian operator associated to $H_{\text{eff,s}}^{BA}$. Next, we introduce the operator $P = \tanh(H'_{\text{eff,s}}/\epsilon)$ whose eigenstates are those of $H'_{\text{eff,s}}$, but whose spectrum $\tanh(E/\epsilon)$ flattens the bulk bands of $H'_{\text{eff,s}}$ and separates them from the zero-energy edge states as the parameter $\epsilon \to 0$. In practice, we want ϵ to be smaller than the bulk gap of $H'_{\text{eff,s}}$ but larger than the energy of the edge states, which is never rigorously zero in finite systems. Introducing then the step function $\theta_j(j')$, which is 1 for $j' \geqslant j$ and 0 otherwise, we can finally define from $H'_{\text{eff,s}}$ the following *topological order parameter*

$$\mathcal{I}(j) = \tfrac{1}{2}\text{Tr}(C[\hat{\theta}_j, P]P), \tag{13}$$

where $\hat{\theta}_j$ is the diagonal operator associated to θ_j. Behind its abstract definition, this local quantity is very useful. It can be shown to be a constant integer (related to the winding number in the periodic case [37]) in regions where $H'_{\text{eff,s}}$ has no zero modes and can only change when crossing regions with zeros modes of $H_{\text{eff,s}}^{BA}$ or $H_{\text{eff,s}}^{BA,\,\dagger}$. In particular, there is a correspondence connecting the index variation $\Delta\mathcal{I} = \mathcal{I}(j_2) - \mathcal{I}(j_1)$ to the number of zero modes of $H_{\text{eff,s}}^{BA}$ localized in the interval $j_1 \leqslant j \leqslant j_2$ minus those of $H_{\text{eff,s}}^{BA,\,\dagger}$ [7,38]. In particular, when $\Delta\mathcal{I} > 0$, this correspondence implies that $H_{\text{eff,s}}^{BA}$ has at least $\Delta\mathcal{I}$ zero modes localized between j_2 and j_1.

If we take $j_1 = 0$, we can prove that $\mathcal{I}(j_1) = 0$ as $\hat{\theta}_{j=0} = \mathbb{1}$. Moreover, as long as the edge state do not invade the whole

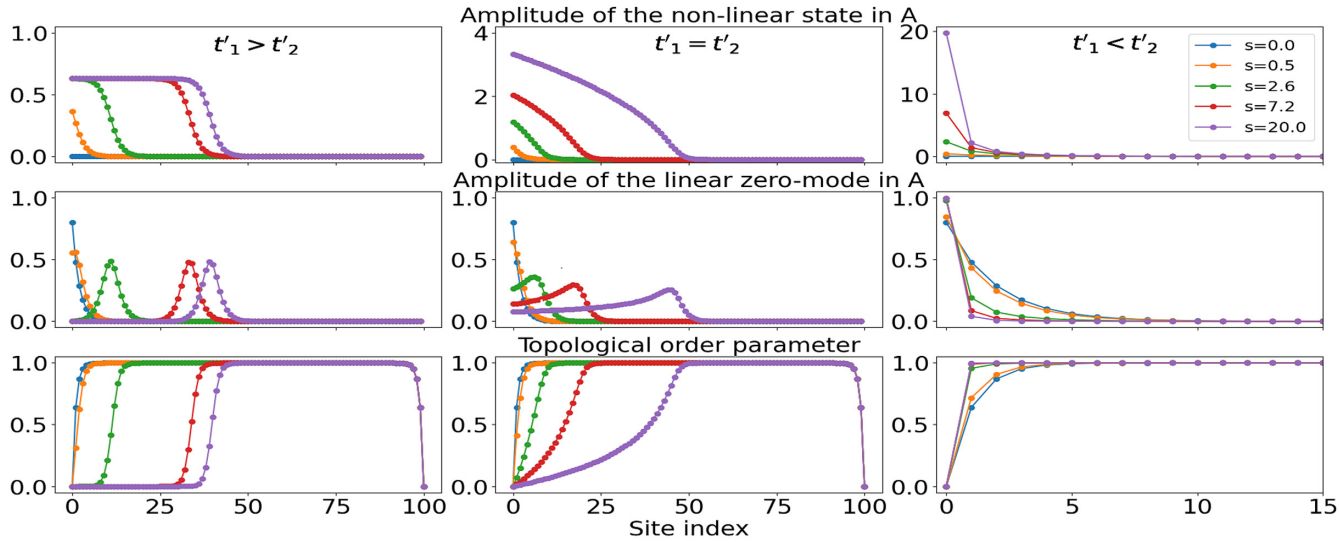

FIG. 2. Numerical resolution of (10) for the left edge modes of the model (14). We work with 100 pairs of sites and $t_1 = 0.6$ $t_2 = 1$ everywhere. For the nonlinear couplings, we take (left) $t'_1 = 1$ $t'_2 = 0$, (center) $t'_1 = 1$ $t'_2 = 1$, and (right) $t'_1 = 0$ $t'_2 = 1$. We draw (up) the amplitude of ψ_s on the A sites (center) the zero-energy state of $H^{AB}_{\text{eff,s}}$ (down) the topological order parameter $I(x)$ where we took $\epsilon = \frac{1}{100}$.

bulk, we have that $H_{\text{eff,s}} \approx H_{\text{eff},0}$ far from the edges. So if we take j_2 far enough from the edges, then $\mathcal{I}(j_2)$ is just the index one would obtain in the bulk of the linearized model at small amplitude. Thus, if we denote $\mathcal{I}$ this topological number, we see that $H^{BA}_{\text{eff,s}}$ is constrained to have at least $\mathcal{I}$ zero modes localized on the left part of the chain. If $|\psi_s\rangle$ is a nonlinear edge mode, it thus implies that we have at least $\mathcal{I}$ possible choices for $|\partial_s \psi_s\rangle$ which are localized and verify (10).

We now apply our nonlinear chiral theory to a concrete model that we solve numerically. As mentioned above, intersites Kerr nonlinearities $H_{\text{inter-Kerr},1}|\psi\rangle = t'_1 \sum_j b_j^3 |j, A\rangle + a_j^3 |j, B\rangle$ are chiral symmetric. For the same reason, the nonlinearities $H_{\text{inter-Kerr},2}|\psi\rangle = t'_2 \sum_j b_j^3 |j+1, A\rangle + a_j^3 |j-1, B\rangle$ are also chiral. However, $H_{\text{inter-Kerr},1}$ reinforces the *intra*cell coupling $|j, A\rangle\langle j, B|$ while $H_{\text{inter-Kerr},2}$ reinforces the *inter*cell coupling $|j+1, A\rangle\langle j, B|$. Those nonlinearities appear, for example, in photonic [39] and electrical systems [25] and even in phononic devices under some approximations [18]. We thus consider a finite SSH chain with such chiral nonlinearities

$$\begin{cases} i\partial_t a_j = (t_1 + t'_1|b_j|^2)b_j + (t_2 + t'_2|b_{j-1}|^2)b_{j-1} \\ i\partial_t b_j = (t_1 + t'_1|a_j|^2)a_j + (t_2 + t'_2|a_{j+1}|^2)a_{j+1}. \end{cases} \tag{14}$$

At small amplitude, the linearization of (14) yields the usual SSH model, and we find $\mathcal{I}(j) = 1$ for $|t_1| < |t_2|$ and j far from the edges. Thus, we predict the existence of a family of chiral nonlinear edge modes $|\psi_s\rangle$ localized on the left A sites of the lattice (a similar argument would also predicts the existence of nonlinear edge modes localized on the right B sites). This is confirmed by our numerical integration of (10) for the model (14) with various choices of parameters (t_1, t_2, t'_1, t'_2) (the first row of Fig. 2). Interestingly, depending on the competition between intercell and intracell nonlinear couplings, we find very different behaviors: When $|t'_1| > |t'_2|$, the amplitude of the edge mode saturates, and the mode becomes a domain wall which invades progressively the bulk. Such a phenomenon was noticed in simulations [18] and an experimental setup [40], both in mechanical lattices. We unveil here the key hidden role of the generalized chiral symmetry to achieve such a nonlinear topological mode. However, this is not the only possible behavior constrained by chiral symmetry. Indeed, when $|t'_1| < |t'_2|$, we find in contrast that the edge mode remains localized at the boundary, with an increasing amplitude concentrated almost on a single site. For the critical value $|t'_1| = |t'_2|$, the edge mode invades the bulk as in the first case, but with a shape that never saturates. Note that these different behaviors as s varies can in principle be probed experimentally by forcing or pumping the system. The origin of these different scenarios can be understood by recalling that the nonlinear modes $|\psi_s\rangle$ are obtained by adding iteratively the zero modes $|\partial_s \psi_s\rangle$ of $H_{\text{eff,s}} = dH^{BA}_{\psi_s}$ whose locations are themselves accounted by the variation of $I(x)$ (Fig. 2). Since dH^{BA}_{ψ} reads

$$\langle j, B| dH^{BA}_{\psi} |\delta\psi\rangle_A = t_{1,\text{eff}}\delta a_j + t_{2,\text{eff}}\delta a_{j+1} \tag{15}$$

with $t_{1,\text{eff}} = t_1 + 3t'_1|a_j|^2$ and $t_{2,\text{eff}} = t_2 + 3t'_2|a_{j+1}|^2$, then, when the a_j's are small enough, $|t_{1,\text{eff}}| < |t_{2,\text{eff}}|$ so that dH^{BA}_{ψ} is in the topological phase with $\mathcal{I}(j) = 1$ in the bulk. But when increasing the amplitude of the a_j's, one may switch to the trivial phase $\mathcal{I}(j) = 0$ where $|t_{1,\text{eff}}| > |t_{2,\text{eff}}|$. If one assumes for simplification that $|a_j| \sim |a_{j+1}| \sim a$, it is clear that the system remains topological even in the high-amplitude regime provided that $|t'_1| < |t'_2|$. In contrast, if $|t'_1| > |t'_2|$, the system undergoes a transition toward a trivial regime where $|t_{1,\text{eff}}| > |t_{2,\text{eff}}|$. Lastly, when $|t'_1| = |t'_2|$, one gets $|t_{1,\text{eff}}| \sim |t_{2,\text{eff}}|$ at high amplitude, leading to a gapless system with $0 < \mathcal{I}(j) < 1$.

As the amplitude a_j actually depends on the position, the system must be though as being divided into two regions separated by some threshold position j_s: The region $j > j_s$ where $|t_{1,\text{eff}}| < |t_{2,\text{eff}}|$ corresponding to the topological phase $I(j) = 1$), and the region $j < j_s$ where $|t_{1,\text{eff}}| > |t_{2,\text{eff}}|$ corresponding to the trivial one, $I(j) = 0$). At the edge of the

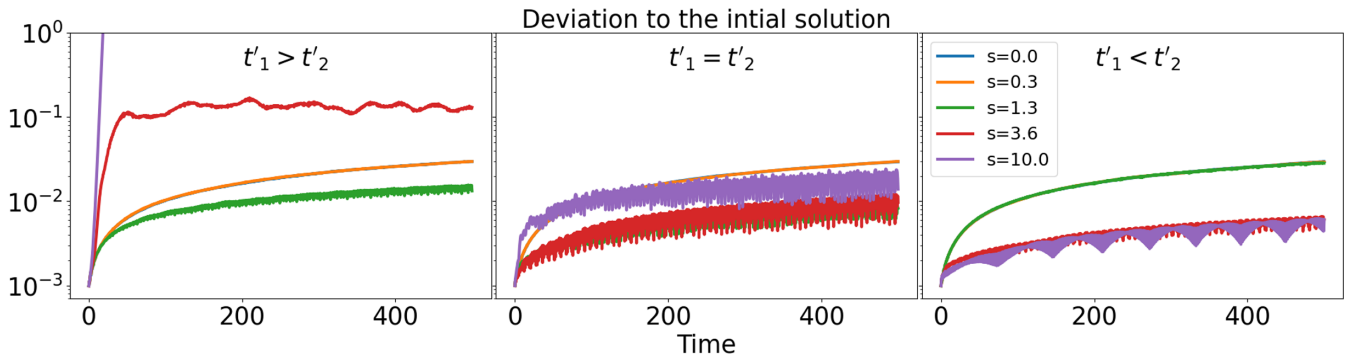

FIG. 3. Evolution of the deviation $\| \, |\psi(t)\rangle - |\psi_s\rangle \, \|$ between the stationary edge states shown in Fig. 2 and an initially perturbed one by a random vector of norm 10^{-3}.

topological phase, $I(j)$ must interpolate between 0 and 1, implying therefore the existence of a zero mode of dH^{BA}_{ψ} nearby. As long as $|t'_1| < |t'_2|$, a transition toward the trivial region cannot occur, and so the zero-energy mode remains localized near the edge. In contrast, if $|t'_1| > |t'_2|$, the effective boundary j_s shifts when increasing the amplitude and dissociates from the physical boundary of the chain. Since $|\partial_s \psi_s\rangle$ is localized around j_s, it shifts toward the bulk while keeping its shape. As a result, $|\psi_s\rangle$ saturates and invades the bulk. The same reasoning applies when $|t'_1| = |t'_2|$, except that j_s becomes an interface between a topological and a *gapless* phase. As a result, $|\partial_s \psi_s\rangle$ decreases slowly far away from j_s into the gapless region, leading to a profile of $|\psi_s\rangle$ which is neither flat ($|t'_1| > |t'_2|$) nor exponential ($|t'_1| < |t'_2|$).

Now that we have established the stationary properties of these topological edge modes, we can look for their nonlinear stability against random perturbations as we did in the nonchiral example. Our results are displayed in Fig. 3. While the energy E_s remains at zero due to the chiral symmetry, we observe that the topological mode is unstable in the case where $|t'_1| > |t'_2|$ about when the plateau of the domain wall is forming, that is from $s \approx 3$–4. In the two other cases, however, we find a relative stability of the edge modes with a deviation that remains relatively small (of order $\approx 10^{-2}$) even at large time $t \gg 1$.

To sum up, we have investigated the fate of topological edge states in 1D nonlinear lattices and showed that those eventually disappear at sufficiently large amplitude, unless the nonlinearities satisfy a generalized chiral symmetry. In that case, a local topological index correctly accounts for the existence and the spatial extension of the nonlinear edge modes, whose actual profile depends on the interplay between the nonlinearities and the underlying topology of the family of linearized Hamiltonians. Our theoretical approach lies on the general hypotheses (i), (ii), and (iii) and then the chiral condition (7) under which the systems (6) and (10) can always be constructed. Therefore, we expect the stationary behaviors we describe to not qualitatively change as long as those general hypothesis are verified, for instance, if one considers nonlinearities in other nonlinear powers than three. On the other side, it is possible that the stability properties of edge modes are more model dependant. An extension of our approach to higher dimension, possibly with other symmetries, is a promising perspective in the search of exotic nonlinear topological states.

APPENDIX: NUMERICAL COMPUTATIONS

In this paper, we shown that if we have an edge solution of $i\partial_t \, |\psi\rangle = H_\psi \, |\psi\rangle$ then we can find other edge solutions by solving the following system of differential equation:

$$(dH_\psi - E_s) \, |\partial_s \psi_s\rangle = (\partial_s E_s) \, |\psi_s\rangle \, . \tag{A1}$$

The most common way to numerically solve this kind of differential system is by using an iterative method like the Runge-Kutta one. The only problem that we have to deal in order to apply these methods is to give a valid solution $(|\delta\psi\rangle \, , \delta E)$ for each s of following linear systems:

$$(dH_\psi - E_s) \, |\delta\psi\rangle = (\delta E) \, |\psi_s\rangle \, . \tag{A2}$$

The vector space of solution of this system can in general be determined by numerical algorithm (the simple one being Gaussian elimination). Once this vector space is determined, we then have to choose one solution in it. This choice is, in general, arbitrary and one can use different method to do it. In general, it is often better to choose solutions for $(|\partial_s u_s\rangle \, , \partial_s E_s)$ which are close of each other for close s as we observe that the Runge-Kutta method is more stable and fast in these cases.

For our numerical simulation, we use the following procedure. First, for $s = 0$, we choose one of the two solutions of the system where $|\delta u\rangle$ is of norm 1 and real. Then iteratively, for the system at time $s + \delta s$, we pick the solution which is of norm 1 and is the closest to the one we choose at time s.

We control the error made by the numerical procedure by measuring the quantity $||E_s \, |\psi_s\rangle - H_{\psi_s} \, |\psi_s\rangle \, ||$ (which should be zero if the procedure is exact). This quantity can be made arbitrarily small at the cost of time of computation. In our example, we are able to obtain $||E_s \, |\psi_s\rangle - H_{\psi_s} \, |\psi_s\rangle \, || < 10^{-11}$ and thus the edge mode created are exact up to a negligible error.

In the chiral case where we do not solve (A1) but the system below, the procedures are almost the same. The only difference is that our variables are only the components of $|\delta\psi\rangle_A$ and not $(|\delta\psi\rangle \, , \delta E)$:

$$H^{BA}_{\text{eff,s}} \, |\partial_s \psi_s\rangle_A = 0. \tag{A3}$$

[1] K. V. Klitzing, G. Dorda, and M. Pepper, New Method for High-Accuracy Determination of the Fine-Structure Constant Based on Quantized Hall Resistance, Phys. Rev. Lett. **45**, 494 (1980).

[2] L. Lu, J. D. Joannopoulos, and M. Soljačić, Topological photonics, Nat. Photon. **8**, 821 (2014).

[3] P. Delplace, J. B. Marston, and A. Venaille, Topological origin of equatorial waves, Science **358**, 1075 (2017).

[4] L. M. Nash, D. Kleckner, A. Read, V. Vitelli, A. M. Turner, and W. T. M. Irvine, Topological mechanics of gyroscopic metamaterials, Proc. Natl. Acad. Sci. USA **112**, 14495 (2015).

[5] Y. Hatsugai, Chern Number and Edge States in the Integer Quantum Hall Effect, Phys. Rev. Lett. **71**, 3697 (1993).

[6] Y. Hatsugai, Edge states in the integer quantum Hall effect and the Riemann surface of the Bloch function, Phys. Rev. B **48**, 11851 (1993).

[7] G. M. Graf and J. Shapiro, The bulk-edge correspondence for disordered chiral chains, Commun. Math. Phys. **363**, 829 (2018).

[8] E. Prodan and H. Schulz-Baldes, *Bulk and Boundary Invariants for Complex Topological Insulators: From K-Theory to Physics* (Springer, Cham, 2016).

[9] M. Seclì, M. Capone, and I. Carusotto, Theory of chiral edge state lasing in a two-dimensional topological system, Phys. Rev. Research **1**, 033148 (2019).

[10] S. Xia, D. Jukić, N. Wang, D. Smirnova, L. Smirnov, L. Tang, D. Song, A. Szameit, D. Leykam, J. Xu, Z. Chen, and H. Buljan, Nontrivial coupling of light into a defect: The interplay of nonlinearity and topology, Light Sci. Appl. **9**, 147 (2020).

[11] D. Smirnova, D. Leykam, Y. Chong, and Y. Kivshar, Nonlinear topological photonics, Appl. Phys. Rev. **7**, 021306 (2020).

[12] M. A. Bandres, S. Wittek, G. Harari, M. Parto, J. Ren, M. Segev, D. N. Christodoulides, and M. Khajavikhan, Topological insulator laser: Experiments, Science **359**, 6381 (2018).

[13] S. Gündoğdu, J. Thingna, and D. Leykam, Edge mode bifurcations of two-dimensional topological lasers, Opt. Lett. **45**, 3673 (2020).

[14] K. Sone, Y. Ashida, and T. Sagawa, Topological synchronization of coupled nonlinear oscillators (unpublished).

[15] D. Leykam and Y. D. Chong, Edge Solitons in Nonlinear-Photonic Topological Insulators, Phys. Rev. Lett. **117**, 143901 (2016).

[16] Y.-P. Ma and H. Susanto, Topological edge solitons and their stability in a nonlinear su-schrieffer-heeger model, Phys. Rev. E **104**, 054206 (2021).

[17] T. Tuloup, R. W. Bomantara, C. H. Lee, and J. Gong, Nonlinearity induced topological physics in momentum space and real space, Phys. Rev. B **102**, 115411 (2020).

[18] R. Chaunsali and G. Theocharis, Self-induced topological transition in phononic crystals by nonlinearity management, Phys. Rev. B **100**, 014302 (2019).

[19] J. R. Tempelman, K. H. Matlack, and A. F. Vakakis, Topological protection in a strongly nonlinear interface lattice, Phys. Rev. B **104**, 174306 (2021).

[20] D. Zhou, D. Z. Rocklin, M. Leamy, and Y. Yao, Topological invariant and anomalous edge states of strongly nonlinear systems (unpublished).

[21] G. Engelhardt, M. Benito, G. Platero, and T. Brandes, Topologically Enforced Bifurcations in Superconducting Circuits, Phys. Rev. Lett. **118**, 197702 (2017).

[22] D. A. Dobrykh, A. V. Yulin, A. P. Slobozhanyuk, A. N. Poddubny, and Y. S. Kivshar, Nonlinear Control of Electromagnetic Topological Edge States, Phys. Rev. Lett. **121**, 163901 (2018).

[23] A. Bisianov, M. Wimmer, U. Peschel, and O. A. Egorov, Stability of topologically protected edge states in nonlinear fiber loops, Phys. Rev. A **100**, 063830 (2019).

[24] M. Ezawa, Topological Toda lattice and nonlinear bulk-edge correspondence (unpublished).

[25] Y. Hadad, J. C. Soric, A. B. Khanikaev, and A. Alu, Self-induced topological protection in nonlinear circuit arrays, Nat. Electron. **1**, 178 (2018).

[26] R. Chaunsali, H. Xu, J. Yang, P. G. Kevrekidis, and G. Theocharis, Stability of topological edge states under strong nonlinear effects, Phys. Rev. B **103**, 024106 (2021).

[27] A. J. Leggett, Bose-Einstein condensation in the alkali gases: Some fundamental concepts, Rev. Mod. Phys. **73**, 307 (2001).

[28] P. Delplace, D. Ullmo, and G. Montambaux, Zak phase and the existence of edge states in graphene, Phys. Rev. B **84**, 195452 (2011).

[29] S. Ryu and Y. Hatsugai, Topological Origin of Zero-Energy Edge States in Particle-Hole Symmetric Systems, Phys. Rev. Lett. **89**, 077002 (2002).

[30] J. M. Combes and L. Thomas, Asymptotic behaviour of eigenfunctions for multiparticle Schrödinger operators, Commun. Math. Phys. **34**, 251 (1973).

[31] A. Michael and S. Warzel, *Random Operators: Disorder Effects on Quantum Spectra and Dynamics*, Graduate Studies in Mathematics (American Mathematical Society, Providence, RI, 2015).

[32] J. C. Butcher, *Numerical Methods for Ordinary Differential Equations* (John Wiley & Sons, New York, 2016).

[33] S. Panda, A. Lahiri, T. K. Roy, and A. Lahiri, Standing waves in a non-linear 1D lattice: Floquet multipliers, Krein signatures, and stability, Phys. D (Amsterdam, Neth.) **210**, 262 (2005).

[34] N. Upadhyaya, B. G. Chen, and V. Vitelli, Nuts and bolts of supersymmetry, Phys. Rev. Research **2**, 043098 (2020).

[35] C. L. Kane and T. C. Lubensky, Topological boundary modes in isostatic lattices, Nat. Phys. **10**, 39 (2014).

[36] J. Attig, K. Roychowdhury, M. J. Lawler, and S. Trebst, Topological mechanics from supersymmetry, Phys. Rev. Research **1**, 032047(R) (2019).

[37] H. Katsura and T. Koma, The noncommutative index theorem and the periodic table for disordered topological insulators and superconductors, J. Math. Phys. **59**, 031903 (2018).

[38] J. Lucien, T. Clément, and D. Pierre, Topological index and bulk-edge correspondence in finite chiral chains (unpublished).

[39] Y. Hadad, A. B. Khanikaev, and A. Alù, Self-induced topological transitions and edge states supported by nonlinear staggered potentials, Phys. Rev. B **93**, 155112 (2016).

[40] B. G.-g. Chen, N. Upadhyaya, and V. Vitelli, Nonlinear conduction via solitons in a topological mechanical insulator, Proc. Natl. Acad. Sci. USA **111**, 13004 (2014).